Ingénierie des Systèmes d'Information
Vol. 31, No. 2, February, 2026, pp. 447-454
Journal homepage: http://iieta.org/journals/isi

A Resource-Efficient YOLO Framework via Discrete Wavelet Transform-Based Image Compression for Plant Disease Detection

Fauzan Masykur[1*], Ellisia Kumalasari[1], Angga Prasetyo[1], Muhammad Arifin[2]

[1] Department of Informatics Engineering, Faculty of Engineering, Muhammadiyah University of Ponorogo, Ponorogo 63471, Indonesia
[2] Information System Department, Faculty of Engineering, Universitas Muria Kudus, Kudus 59300, Indonesia

Corresponding Author Email: fauzan@umpo.ac.id

https://doi.org/10.18280/isi.310213

Received: 26 September 2025
Revised: 5 December 2025
Accepted: 13 December 2025
Available online: 28 February 2026

Keywords:
Discrete Wavelet Transform, YOLO, image compression, resource-efficient object detection, plant disease detection, agricultural image analysis, lightweight models

ABSTRACT

Efficient processing of large-scale agricultural image data remains a critical challenge for real-time plant disease detection systems, particularly in resource-constrained environments. This study proposes a resource-efficient object detection framework that integrates Discrete Wavelet Transform (DWT)-based image compression with the YOLO detection algorithm to reduce data transmission and storage overhead while preserving detection performance. The proposed approach applies multi-level wavelet decomposition and lossless encoding to compress input images prior to model training and inference. Experimental results demonstrate that the method achieves substantial data reduction, with file size compression ratios of up to 99.7%, while maintaining high visual fidelity (PSNR: 44.8–63.3 dB; MSE: 0.001–0.36). Despite aggressive compression, the detection model retains stable performance, achieving an mAP of 0.281 and an average F1-score of 0.34, with an improved inference speed of 23.56 ms. These results indicate that DWT-based compression can effectively reduce computational resource requirements without significantly degrading object detection capability. The proposed framework provides a practical solution for deploying lightweight and scalable plant disease detection systems in real-world agricultural monitoring scenarios.

1. INTRODUCTION

Food self-sufficiency has become a strategic objective in many countries, as it is closely linked to food security, economic resilience, and agricultural sustainability [1, 2]. Achieving this requires the availability of staple foods such as rice, corn, and wheat, as well as fruit and other essential commodities. The goals of food self-sufficiency include ensuring national food security, reducing global dependence, improving farmer welfare, and maintaining domestic stability.

Collaboration across sectors is vital to achieve these aims. This involves strategic policies from authorities, effective implementation, and efforts to enhance farmer knowledge. Rice is central to these efforts, as it is the primary staple for Indonesians and people worldwide. Indonesia is now the fourth largest rice producer, after China, India, and Bangladesh [3, 4].

Image processing in agriculture requires efficient methods due to the large amount of data and the need for on-the-spot analysis [5]. The Discrete Wavelet Transform (DWT) provides an image compression solution that preserves essential structure by separating low- and high-frequency components [6]. This approach allows for image downscaling without losing the fundamental information needed to recognize plants with diverse and complex shapes and textures.

On the other hand, modern object detection algorithms such as YOLO have proven fast and accurate at recognizing various types of plant objects, but their performance depends heavily on the image quality and size. Therefore, integrating a DWT coefficient-based compression method as a pre-processing step before YOLO is a promising solution to reduce computational resource usage without compromising detection accuracy [6-9]. This study aims to evaluate the effectiveness of combining DWT and YOLO to produce a lighter, more efficient, yet still accurate plant detection system.

One widely used object detection algorithm today is You Only Look Once (YOLO) [10, 11]. It has an average inference speed of 27.59 ms and a precision rate of 77.3% [12]. The YOLO algorithm has been applied in various sectors for object detection, including plant disease detection [13, 14], medical image detection [15-17], small object detection [18, 19], and the military [20]. YOLOv10 is a highly accurate algorithm for predicting object categories and locations in images with low latency. Several versions of YOLO have become leading object detection technologies due to their performance and efficiency. However, YOLO's development has a shortcoming: its dependence on Non-Maximum Suppression (NMS) and inefficient architecture design, both of which limit YOLOv10's performance. To address these issues, YOLOv10 introduces a consistent dual assignment mechanism for holistic model training on NMS. This achieves a balance

between model efficiency and accuracy [10]. Figure 1 shows the YOLOv10 architecture, which includes regression and classification for both one-to-many and one-to-one heads.

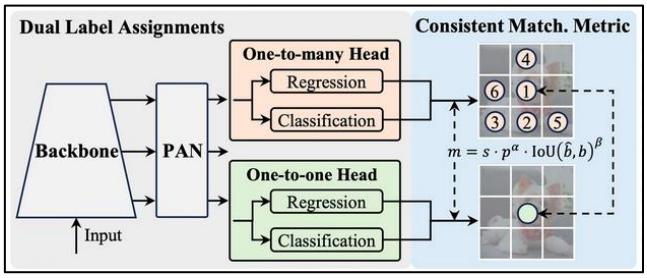

Figure 1. YOLO architecture

However, YOLO still has weaknesses in data transmission and storage due to its high resource requirements. To address this, innovations are needed that reduce the size of monitored image datasets while retaining their critical information. One solution is to use image compression techniques based on DWT, which are particularly well-suited to the JPEG image format. This process can be followed by Huffman coding. As a result, the image retains critical information, but its size is reduced and it is more efficient for further processing [8, 21, 22]. Plant image compression for disease diagnosis requires lightweight and flexible imagery. The method should not reduce or damage the information within the image [7, 23, 24].

Plant images captured by drones and CCTV typically produce large image files. These require more effective storage and transmission capacity. Reducing image file size impacts cost, speed, and simplifies database management. However, using the wrong image compression technique can result in the loss or corruption of information in the image. Therefore, appropriate compression methods are needed to prevent the loss of critical information. The DWT image compression technique is followed by reduction and Huffman coding operations to produce a lossless type of compressed image. The DWT has its coefficients extracted and mapped to the nearest integer [7]. Four sub-bands of the DWT are combined with 3 × 3 windows used as pivot elements. Figure 2 shows the framework of the DWT with Huffman coding.

The JPEG static image compression standard is widely used in disease diagnosis. This is because it can encode discrete transformations and use advanced entropy coding. The coding is also easy to implement on hardware [25]. Figure 3 shows how images are divided into 8 × 8 blocks, with each block becoming 64 DWT coefficients. Most of these coefficient amplitudes are zero or near zero. Lossless coding is based on the statistical properties of the quantification coefficient. The available entropy coding method is arithmetic Huffman coding. Huffman coding needs at least one table specified by the application. For decoding, the Huffman step uses an entropy decoder. This involves quantification, Huffman, and inverse arithmetic operations [26].

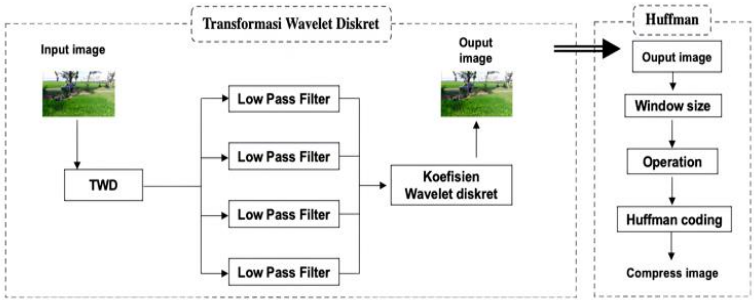

Figure 2. Discrete Wavelet Transform (DWT) framework and Huffman coding

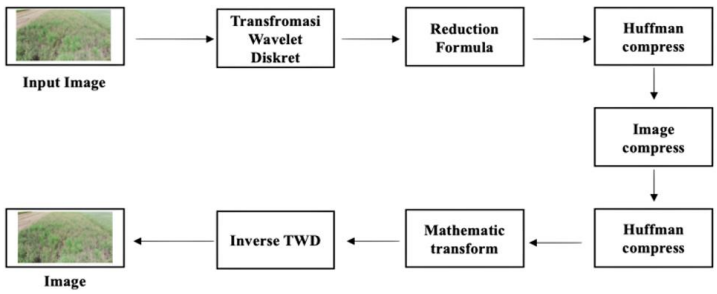

Figure 3. Block diagram of Huffman compression

2. LITERATURE REVIEW

2.1 Lossy compression Discrete Wavelet Transform

The wavelet transform is a signal-processing method that analyzes data based on frequency differences and determines the locations of those frequencies. Applications include watermarking [27], health detection [8], sensing [28], and solving differential equations [29]. The approach involves two main stages: the DWT separates signal components into low- and high-frequency components, and the Inverse Discrete Wavelet Transform (IDWT) reconstructs the original signal.

The DWT stage is typically used to reduce image size by quantizing high-frequency components. This process enhances the efficiency of data storage and transmission. The IDWT stage restores the transformed image components to their original form. For compressed images, DWT, IDWT, and

dequantization enable image reconstruction. This maintains image quality close to the original. Thus, the wavelet transform plays a significant role in image processing. It is particularly useful in data compression and image quality restoration.

Originally developed to analyze non-stationary signals via multi-resolution analysis, the wavelet transform allows observation of frequency components at several resolution levels. Quantization of DWT coefficients introduces limited information loss; however, when combined with appropriate encoding schemes, high reconstruction fidelity can be preserved. For storage and transmission efficiency, studies use canonical Huffman coding or combine wavelet filtering with Huffman coding [6, 30].

In the continuous wavelet transform, the scale (a) and translation (b) parameters vary continuously, resulting in high computational complexity. The DWT addresses this by restricting a and b to discrete multiples of two, enabling more efficient analysis using specific values. DWT processes large data sets faster and more effectively. Eq. (1) defines the mathematical formulation of the wavelet function based on discrete scale and translation parameters [31].

$$\varphi_{a,b}(t) = \frac{1}{\sqrt{|a|}}\varphi\left(\frac{t-b}{a}\right) \quad (1)$$

where, $\varphi_{a,b}(t)$ denotes the wavelet coefficients at scale a and shift a, with $x(t)$ as the input signal and $\varphi(t)$ as the wavelet function. Parameter a governs compression /dilation, while b determines the position in the time domain. Expanding Eq. (1) by substituting several parameters, $a = 2^r$ and $b = k.\ 2^r$, then produces Eq. (2).

$$\varphi_{r,k}(t) = \frac{1}{\sqrt{|2^r|}}\varphi\left(\frac{t-k.2^r}{2^r}\right) \quad (2)$$

Description $\varphi_{r,k}(t)$ is a discrete wavelet function with r as the scale and k as the translation. Substitution of Eq. (2) into the continuous wavelet transform produces the discrete form, as shown in Eq. (3).

$$DWT_{r,k} = \frac{1}{\sqrt{|2^r|}}\int_{-\infty}^{+\infty} x(t)\varphi\left(\frac{t-k.2^r}{2^r}\right) \quad (3)$$

The calculation of the discrete wavelet coefficients $DWT_{r,k}$ is performed by applying a discrete scale parameter 2^r and a translation $k.2^r$ to the signal $x(t)$ through the wavelet function $\varphi(t)$. This formulation represents the result of substituting the continuous wavelet transform into a discrete form, designed to optimize computational efficiency for large-scale datasets.

2.2 YOLO object detection

Object detection is a key area of computer vision, aiming to recognize and locate objects in images or videos. The YOLO algorithm was developed as a one-stage detector that formulates object detection as a single regression, enabling it to predict object class and bounding box coordinates directly in a single process. This approach makes YOLO faster and more efficient than two-stage methods such as R-CNN and its derivatives, making it widely used in various applications requiring real-time detection [32, 33].

YOLOv8 is one of the latest versions, introduced by Ultralytics in 2023. YOLOv8 brings several innovations. It uses a C2f module in the backbone for more efficient feature extraction. It combines a Feature Pyramid Network (FPN) and a Path Aggregation Network (PAN) in the neck for better multi-scale detection. It also implements an anchor-free head for direct object prediction, removing the need for anchor boxes. These architectural improvements enhance detection accuracy and computational efficiency, making YOLOv8 suitable for real-time vision applications. Thus, it is relevant for fields from intelligent surveillance to industrial manufacturing [34, 35].

3. METHODOLOGY

3.1 Material

This research utilized several tools to support the implementation of this activity. Plant image acquisition was performed using several cameras with varying specifications. Table 1 shows the equipment used for image acquisition. Various types of image acquisition equipment were used to evaluate the effectiveness of image compression as a training dataset for object detection models.

The equipment used has different strengths and weaknesses; therefore, image acquisition requires different equipment. The image acquisition angles are also varied, with various angles (side, top, and oblique). Table 2 presents a sample dataset from the acquisition results. The example images consist of three types of plants (banana, mango, and guava).

Table 1. List of image acquisition equipment

No.	Device	Specification
1	Samsung A25 5G	● Technology: Super AMOLED 120 Hz ● Resolution: FHD+ ● Rear Camera Resolution: 50.0 MP + 8.0 MP + 2.0 MP ● Rear Camera Zoom: Digital Zoom up to 10x ● Front Camera Resolution: 13.0 MP ● ISO Range: 100-3200 ● Video Resolution: 3840 × 2160 (30fps | 125fps | 24fps) ● Shutter Speed: 32~1/8000s ● Format Video: MP4 ● Photo Format: JPG, JPG+DNG
2	Fimi X8 Mini	● Main Camera: 64 MP + 8 MP + 2 MP ● Video: 4K@30fps, 1080p@30/60/120/480fps, gyro-EIS ● Selfie Camera: 32 MP, f/2.4, 22 mm (wide), 1/2.74", 0.8 µm ● Resolution: 2460 × 1080 ● Refresh Rate: Up to 90Hz
3	Oppo Reno 11 F	● Rear Camera: ➢ 50 MP main camera ➢ 8 MP ultra-wide camera ➢ 2 MP macro camera ● Front Camera: 8 MP (f/2.1)
4	Xiaomi Redmi Note 12	

3.2 Research stages

Figure 4 shows the stages of this research, which comprises six main, interconnected phases. First, image acquisition is performed using drones and CCTV as devices for compiling the plant dataset. Next, the image augmentation stage enhances images through processes such as resizing, rotating,

cropping, and flipping, which helps prevent overfitting during model training. Following augmentation, image compression and Huffman processing take precedence in the first year, as dataset images are compressed and encoded to simplify and reduce their size while preserving important information. This process also aims to decrease server resource usage when integrating the object detection model. Subsequently, labeling is carried out using several software programs, including YOLO-Mark, LabelImg, Computer Vision Annotation Tool (CVAT), and Roboflow.

Table 2. Plant image dataset

Plant Type	Acquisition Equipment	Image
Banana	Samsung A25	
	Fimi X8 Mini	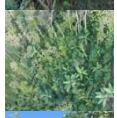
Guava	Samsung A25	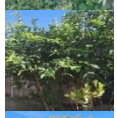
	Fimi X8 Mini	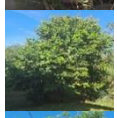
Mango	Samsung A25	
	Fimi X8 Mini	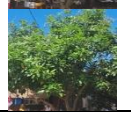

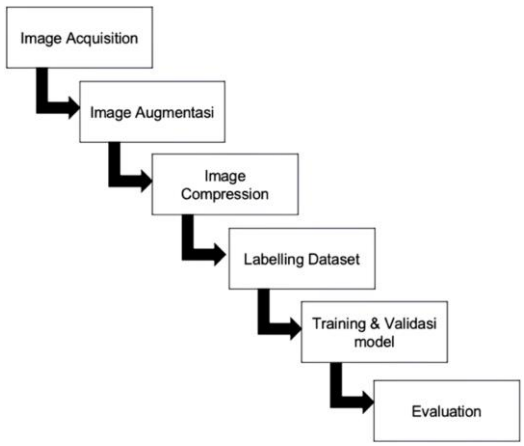

Figure 4. Research stage

LabelImg, YOLO-Mark, CVAT, and Roboflow Annotate differ significantly in their functionality and complexity. LabelImg is a simple, fast-to-use tool suitable for small projects because it supports only bounding-box annotation and lacks collaboration and automation features. YOLO-Mark is a dedicated tool for the YOLO format, providing YOLO-focused labeling with a minimalist interface, but its annotation features are limited and less flexible for complex projects. CVAT is a comprehensive web-based platform that supports many annotation types, including polygons, videos, and teamwork, making it suitable for large projects or complex datasets, though it requires more complex configuration. Roboflow Annotate offers an integrated, cloud-based solution with powerful automation, modern collaboration, and robust dataset management, making it suitable for end-to-end workflows. However, some premium features require payment and depend on cloud services.

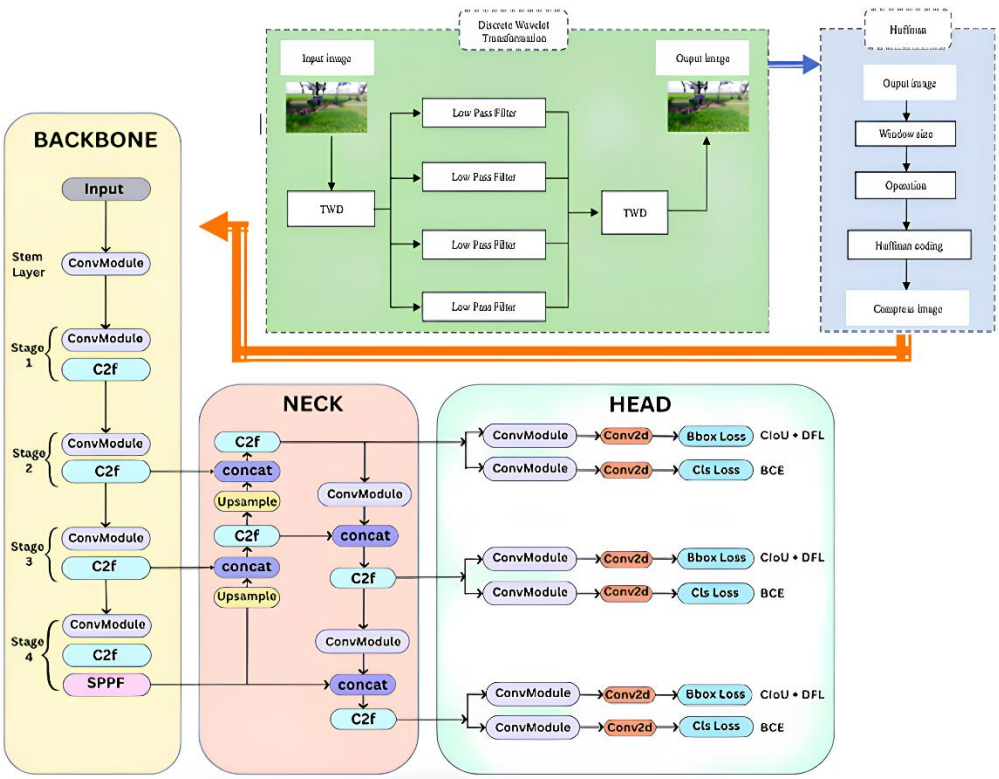

Figure 5. Working diagram of image compression and object detection algorithm

In this study, labeling involved three classes of plants: banana, mango, and guava, with 200 images each, for a total of 600 images. After labeling, model training and validation are conducted on Google Colab with the yolo model, followed by validation from agricultural experts. Finally, server integration is completed, enabling the training result model to be utilized for object detection and determining agricultural land areas for crop yield prediction.

3.3 Purpose method

The objective of this research is to reduce the size of the image dataset without reducing the important information from the image. A smaller image size will speed up the object detection model in determining the object. The image dataset was compressed using the Huffman coding method, preceded by a DWT. This method was chosen because Huffman coding is a type of lossless image compression where important image information is not lost. Huffman code works by encoding image pixels based on their frequency of occurrence. Pixel codes that rarely appear get longer bit codes, while pixel codes that appear frequently get shorter bit codes, thereby reducing storage space. Figure 5 shows the performance scheme of the research in reducing the image dataset. The proposed performance scheme is to insert image compression using the Huffman coding method with a lossless type before the image dataset is used as a model training dataset. The acquired image is first resized without losing important information. The performance diagram scheme of the proposed method is a combination of research by Dsilva et al. [36].

4. RESULT AND DISCUSSION

Image compression is a crucial process in digital image processing that reduces data size without significantly compromising visual quality. One widely used method is the DWT due to its ability to represent images in the frequency domain with multi-resolution analysis. Through the decomposition process, DWT divides the image into low-frequency components that retain the main information and high-frequency components that contain fine details, thus enabling efficient data reduction. Table 3 presents sample image compression results, including PSNR and MSE values.

The results of the dataset image compression in Table 3 show that the image compression results produce different values. The dataset image sampling is the result of camera acquisition with different specifications, as shown in Table 1. The largest difference in compression results is in data 9, which is the result of acquisition from the FIMI X8 Mini drone camera. Based on the image compression results, the next step is to detect objects using the YOLO object detection algorithm. The dataset, in the form of plant images, will be classified into three classes: banana, mango, and guava. In this study, the dataset labeling utilizes two software tools, namely the CVAT and LabelImg.

Table 4 shows the resulting images from image compression (before and after compression). The images before and after compression show very little difference. Visually, the original image has slightly sharper details in the texture of the banana leaf and stem, with smoother color transitions. After compression, some fine details appear slightly reduced and object edges feel softer, but the main plant structure is maintained. The quantitative analysis results also support this observation, showing minimal pixel differences, while the very high SSIM value indicates that the structures of the two images are almost identical. Overall, the compression process does not destroy important information in the image and is still very suitable for use in object detection processes such as YOLO, because the main shape and pattern of the plant are well preserved.

Table 3. Dataset image compression results

Data	Size		MSE	PSNR	Ratio
	Before (Kb)	After (Kb)			
1	3435	1341	0.035	55.7	39
2	3610	1422	0.04	54.8	39.3
3	3875	1541	0.05	53.9	39.7
4	3974	1574	0.05	53.5	39.6
5	172.7	172.3	0.36	44.8	99.7
6	168.2	165.3	0.09	50.8	98.2
7	4603	1586	0.01	58.9	34.4
8	4135	1378	0.01	59.6	33.3
9	3646	1186	00.01	61.1	32.5
10	4175	1374	0.01	59.5	32.9
11	3304	1103	0.01	62	33.3
12	3907	1028	0.001	63.3	33.1
13	4246	1384	0.01	59.06	32.6
14	257	251	0.03	56.2	98
15	267	263	0.03	55.1	98.5
16	253	250	0.03	55.3	98.8

Note: MSE = mean squared error; PSNR = peak signal-to-noise ratio.

Table 4. Comparison of images before and after image compression

Before	After
	

The results of the classification model evaluation (Figure 6), based on the confusion matrix, show an overall accuracy of 25.6%, with macro-average precision, recall, and F1-score values of 25.4%, 24.5%, and 24.2%, respectively. The main errors occurred in the model's tendency to classify fruit objects as background objects, as well as overlapping predictions between fruit classes, particularly between mango and guava. These findings indicate the need for improvements to the training data and model architecture to more accurately distinguish the visual characteristics of each class.

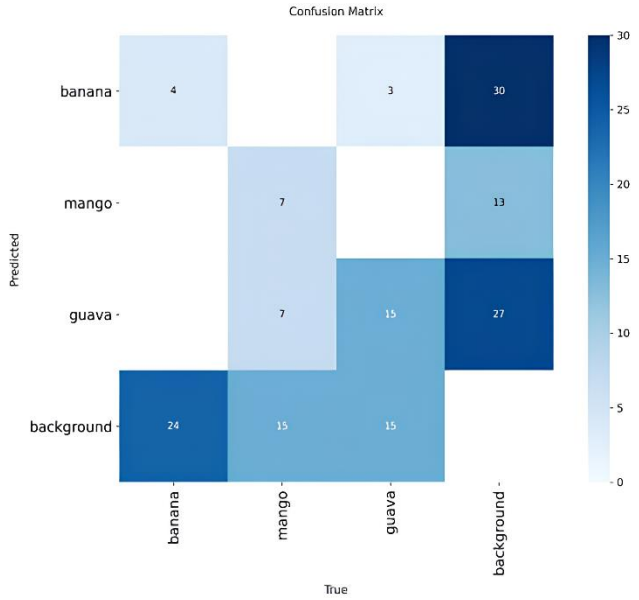

Figure 6. Confusion matrix

Figure 7, a recall-confidence graph, shows that recall decreases as the confidence threshold increases. The guava class performed best, with a relatively higher recall compared to the banana and mango classes, whose recalls declined rapidly at higher thresholds. Overall, the model achieved a recall of 0.69 at a threshold of 0.0; however, performance decreased significantly as the confidence threshold was increased. This confirms the trade-off between recall and prediction confidence.

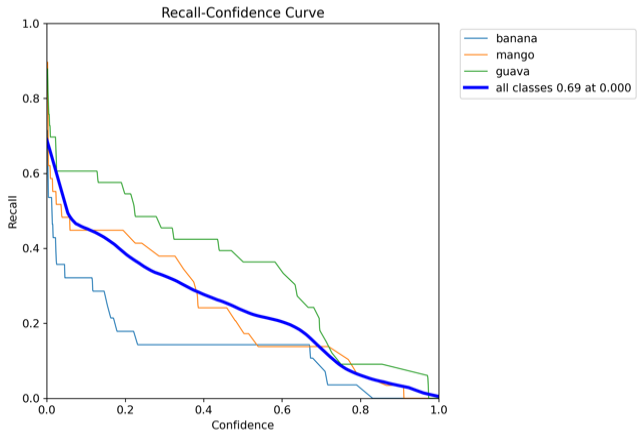

Figure 7. Recall graph

Figure 8, a precision-confidence graph, shows that precision values increase as the confidence threshold increases. The guava class has the highest precision (> 0.8), followed by mango, which shows moderate performance, while banana exhibits very low precision. Overall, the model achieved a precision of 1.00 at a threshold of 0.961, although this potentially reduces recall. These results confirm the trade-off between precision and recall in model performance.

Figure 9 shows the precision-recall curve, showing that the guava class performed best (AP = 0.416), followed by mango (AP = 0.340), and banana performed the lowest (AP = 0.086). The average mAP@0.5 value of 0.281 indicates that the model's performance is still low and requires improvement through improvements to the dataset and model architecture.

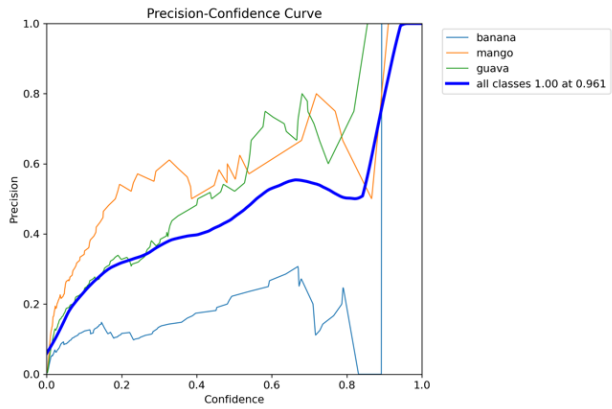

Figure 8. Precision value

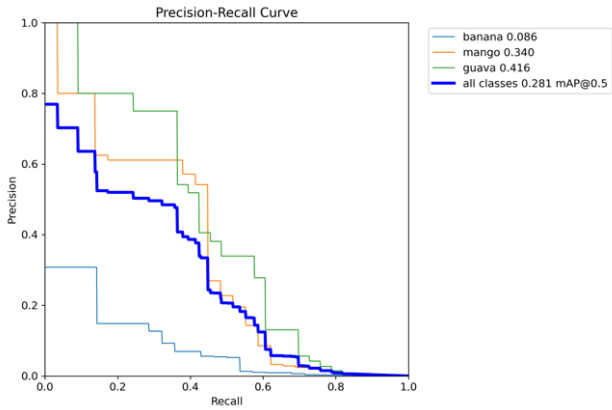

Figure 9. Precision-recall graph

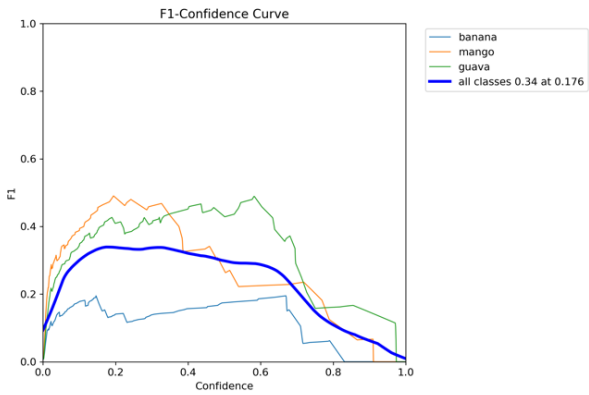

Figure 10. F1 graph

Figure 10 is an F1-Confidence graph showing the variation in F1-score values against the confidence threshold. In general, the model achieved the highest average F1-score of 0.34 at a threshold of 0.176. The guava and mango classes performed relatively better than the banana class, with their respective F1 peaks approaching 0.5. Meanwhile, the banana class tended to have low stability and the lowest F1-score along the curve. These results indicate that model performance is more consistent across certain classes.

5. CONCLUSION

The results show that image compression can reduce file

size by up to 99.7% while maintaining visual quality, as indicated by high PSNR values (44.8–63.3 dB) and low MSE (0.001–0.36). The quality of the compressed images is shown to support the detection model's performance, as reflected in the evaluation curve. The precision-recall curve produces a mAP@0.5 value of 0.281, while the F1-confidence curve shows an average F1 value of 0.34, indicating a balance between precision and recall at a certain confidence level. In addition, the performance variation across classes (banana, mango, guava) indicates that good image quality after compression contributes to differences in detection rates. Overall, these results confirm that image compression with minimal distortion is not only efficient for storage but also maintains the accuracy and consistency of image-based object detection models. In the future, this research can be expanded by including more datasets, both in terms of quantity and class.

ACKNOWLEDGMENT

The author would like to express his gratitude to the Ministry of Higher Education, Science, and Technology for the research funding support under the Regular Fundamental Research (PFR) scheme in 2025. He also expressed his gratitude to the Muhammadiyah University of Ponorogo and the Institute for Research and Community Service (LPPM) of the same university for providing assistance and facilitation in the implementation of this research. He also expressed his sincere appreciation to all parties who have assisted, both directly and indirectly, in enabling the successful completion of the research and writing of this article.

REFERENCES

[1] Tleuberdinova, A., Nurlanova, N., Alzhanova, F., Salibekova, P. (2025). Food security and self-sufficiency as a factor of country's sustainable development: Assessment methods and solutions. Discover Sustainability, 6(1): 50. https://doi.org/10.1007/s43621-025-00849-y

[2] Astuti, S.J.W., Putra, A.P. (2024). Dynamics of food self-sufficiency and stunting: Evidence Jember Regency Indonesia. In Iapa Proceedings Conference, pp. 956-974. https://doi.org/10.30589/proceedings.2024.1170

[3] Sitaresmi, T., Hairmansis, A., Widyastuti, Y., Rachmawati. (2023). Advances in the development of rice varieties with better nutritional quality in Indonesia. Journal of Agriculture and Food Research, 12: 100602. https://doi.org/10.1016/j.jafr.2023.100602

[4] U.S. Department of Agriculture. (2024). Production-Rice, 2024. https://fas.usda.gov/data/production/commodity/0422110.

[5] Joshi, P., Sandhu, K.S., Singh Dhillon, G., Chen, J., Bohara, K. (2024). Detection and monitoring wheat diseases using unmanned aerial vehicles (UAVs). Computers and Electronics in Agriculture, 224: 109158. https://doi.org/10.1016/j.compag.2024.109158

[6] Ranjan, R. (2020). Canonical Huffman coding based image compression using wavelet. Wireless Personal Communications, 117(3): 2193-2206. https://doi.org/10.1007/s11277-020-07967-y

[7] Geetha, V., Anbumani, V., Parameshwaran, R., Gomathi, S. (2022). Savitzky Golay and KPCA based optimal discrete wavelet transform architecture for image compression. Microprocessors and Microsystems, 91: 104511. https://doi.org/10.1016/j.micpro.2022.104511

[8] Palanisamy, K., Viswanathan, P. (2023). An empirical selection of wavelet for near-lossless medical image compression. Current Medical Imaging Reviews, 20: e0230330. https://doi.org/10.2174/1573405620666230330113833

[9] Chen, A., Gui, J., Ma, X., Liu, J., Jiang, Z., Song, Q. (2023). Compression of color digital hologram using wavelet thresholds and two-times quantization. Optics Communications, 537: 129439. https://doi.org/10.1016/j.optcom.2023.129439

[10] Wang, A., Chen, H., Liu, L., Chen, K., Lin, Z., Han, J., Ding, G. (2024). YOLOv10: Real-time end-to-end object detection. arXiv preprint arXiv:2405.14458. https://doi.org/10.48550/arXiv.2405.14458

[11] Furlanetto, R.H., Boyd, N.S., Buzanini, A.C. (2025). Multi-crop plant counting and geolocation using a YOLO-powered GUI system. Smart Agricultural Technology, 11: 100994. https://doi.org/10.1016/j.atech.2025.100994

[12] Masykur, F., Adi, K., Nurhayati, O.D. (2023). Approach and analysis of Yolov4 algorithm for rice diseases detection at different drone image acquisition distances. TEM Journal, 12(2): 928-935. https://doi.org/10.18421/TEM122-39

[13] Rajagopal, M., Kayikci, S., Abbas, M., Sivasakthivel, R. (2024). A novel technique for leaf disease classification using Legion Kernels with parallel support vector machine (LK-PSVM) and fuzzy C means image segmentation. Heliyon, 10(12): e32707. https://doi.org/10.1016/j.heliyon.2024.e32707

[14] Thorat, T., Patle, B.K., Kashyap, S.K. (2023). Intelligent insecticide and fertilizer recommendation system based on TPF-CNN for smart farming. Smart Agricultural Technology, 3: 100114. https://doi.org/10.1016/j.atech.2022.100114

[15] Md Ali, M.A., Abidin, M.R., Nik Muhamad Affendi, N.A., Abdullah, H., R.Rosman, D., Barud'din, N., Kemi, F., Hayati, F. (2021). Classification of chest radiographs using novel anomalous saliency map and deep convolutional neural network. IIUM Engineering Journal, 22(2): 234-248. https://doi.org/10.31436/iiumej.v22i2.1752

[16] Kumar, A. (2022). RYOLO v4-tiny: A deep learning based detector for detection of COVID and non-COVID pneumonia in CT scans and X-ray images. Optik, 268: 169786. https://doi.org/10.1016/j.ijleo.2022.169786

[17] Hussein, S.S., Rashidi, C.B.M., Aljunid, S.A., Salih, M.H., Abuali, M.S., Khaleel, A.M. (2023). Enhancing cardiac arrhythmia detection in WBAN Sensors through supervised machine learning and data dimensionality reduction techniques. Mathematical Modelling of Engineering Problems, 10(6): 2051-2062. https://doi.org/10.18280/mmep.100615

[18] Dai, C., Song, T., Chen, Q., Gong, H., Yang, B., Song, G. (2025). FSIC: Frequency-separated image compression for small object detection. Digital Signal Processing, 156: 104822. https://doi.org/10.1016/j.dsp.2024.104822

[19] Nghiem, V.Q., Nguyen, H.H., Hoang, M.S. (2025). LEAF-YOLO: Lightweight edge-real-time small object

detection on aerial imagery. Intelligent Systems with Applications, 25: 200484. https://doi.org/10.1016/j.iswa.2025.200484
[20] Kwon, H., Lee, S. (2024). Novel rifle number recognition based on improved YOLO in military environment. Computers, Materials & Continua, 78(1): 249-263. https://doi.org/10.32604/cmc.2023.042466
[21] Thomas, S., Krishna, A., Govind, S., Sahu, A.K. (2025). A novel image compression method using wavelet coefficients and Huffman coding. Journal of Engineering Research, 13(1): 361-370. https://doi.org/10.1016/j.jer.2023.08.015
[22] Urban, C.E.R., da Rosa, M.M.A., da Costa, E.A.C. (2026). Energy-efficient discrete Haar Wavelet Transform architectures exploring approximate adders for high-quality image compression and reconstruction. Future Generation Computer Systems, 174: 107999. https://doi.org/10.1016/j.future.2025.107999
[23] Rajasekar, D., Theja, G., Prusty, M.R., Chinara, S. (2024). Efficient colorectal polyp segmentation using wavelet transformation and AdaptUNet: A hybrid U-Net. Heliyon, 10(13): e33655. https://doi.org/10.1016/j.heliyon.2024.e33655
[24] Muthulingam, G.A., Parvathy, V.S. (2023). A novel bacterial foraging optimization based multimodal medical image fusion approach. Applied Science and Engineering Progress, 16(3): e2023030. https://doi.org/10.14416/j.asep.2023.03.004
[25] Charrier, M., Cruz, D.S., Larsson, M. (1999). JPEG2000, the next millennium compression standard for still images. In Proceedings IEEE International Conference on Multimedia Computing and Systems, Florence, Italy, pp. 131-132. https://doi.org/10.1109/mmcs.1999.779134
[26] Yuan, S., Hu, J. (2019). Research on image compression technology based on Huffman coding. Journal of Visual Communication and Image Representation, 59: 33-38. https://doi.org/10.1016/j.jvcir.2018.12.043
[27] Alsabaan, M., Faheem, Z.B., Zhu, Y., Ali, J. (2025). Image watermarking algorithm base on the second order derivative and discrete wavelet transform. Computers, Materials & Continua, 84(1): 491-512. https://doi.org/10.32604/cmc.2025.064971
[28] Ye, G., Du, S., Huang, X. (2023). Image compression-hiding algorithm based on compressive sensing and integer wavelet transformation. Applied Mathematical Modelling, 124: 576-596. https://doi.org/10.1016/j.apm.2023.08.015
[29] Adhikary, S., Varalasetty, S.D., Nadella, S.T., Ghosh, A., Nandi, S. (2024). PrivLet: A differential privacy and inverse wavelet decomposition framework for secure and optimized hemiplegic gait classification. Biomedical Signal Processing and Control, 96: 106577. https://doi.org/10.1016/j.bspc.2024.106577
[30] Sharma, S.J., Gupta, R. (2025). Deep learning based EEG based mental workload detection with discrete wavelet transform and Welch's power spectral density. Procedia Computer Science, 260: 134-141. https://doi.org/10.1016/j.procs.2025.03.186
[31] Chen, D., Wan, S., Xiang, J., Bao, F.S. (2017). A high-performance seizure detection algorithm based on discrete wavelet transform (DWT) and EEG. PLos One, 12(3): e0173138. https://doi.org/10.1371/journal.pone.0173138
[32] Redmon, J., Divvala, S., Girshick, R., Farhadi, A. (2016). You Only Look Once: Unified, real-time object detection. In 2016 IEEE Conference on Computer Vision and Pattern Recognition (CVPR), Las Vegas, NV, USA, pp. 779-788. https://doi.org/10.1109/cvpr.2016.91
[33] Jin, H., Ren, S., Li, S., Liu, W. (2025). Research on mine personnel target detection method based on improved YOLOv8. Measurement, 245: 116624. https://doi.org/10.1016/j.measurement.2024.116624
[34] Jocher, G., Chaurasia, A., Qiu, J., Stoken, A. (2023). YOLO by ultralytics. GitHub Repository. https://github.com/ultralytics/ultralytics.
[35] Feng, F., Hu, Y., Li, W.P., Yang, F.Y. (2024). Improved YOLOv8 algorithms for small object detection in aerial imagery. Journal of King Saud University-Computer and Information Sciences, 36(6): 102113. https://doi.org/10.1016/j.jksuci.2024.102113
[36] Dsilva, L.R., Tantri, S.H., Sampathila, N., Mayrose, H., Muralidhar Bairy, G., Belurkar, S., Saravu, K., Chadaga, K., HafeezBaig, A. (2024). Wavelet scattering and object detection-based computer vision for identifying dengue from peripheral blood microscopy. International Journal of Imaging Systems and Technology, 34(1): e23020. https://doi.org/10.1002/ima.23020